Available online at www.sciencedirect.com
SCIENCE DIRECT®
Journal of Power Sources 140 (2005) 129–138
JOURNAL OF POWER SOURCES
www.elsevier.com/locate/jpowsour

# Simulated low-earth-orbit cycle-life testing of commercial laminated lithium-ion cells in a vacuum

Xianming Wang*, Chisa Yamada, Hitoshi Naito, Saburo Kuwajima

*Institute of Space Technology and Aeronautics, Japan Aerospace Exploration Agency, Tsukuba Space Center, Sengen 2-1-1, Ibaraki 305-8505, Japan*

Received 16 June 2004; received in revised form 6 August 2004; accepted 11 August 2004
Available online 7 October 2004

**Abstract**

We tested the life cycle of commercial laminated lithium-ion cells with both liquid (LE cells) and polymer (PE cells) electrolytes by simulating a satellite's low earth orbit (LEO) operation under various environmental conditions to develop a power storage system for microsatellites. We completed 4000 cycles, corresponding to about 8 months of LEO satellite operation. The LE cell initially exhibited better performance than the PE cell in a normal atmosphere. However, the LE cell began to expand in a vacuum (about 20 Pa), accompanied by capacity loss and voltage decline at the end of the discharge. In contrast, the PE cell exhibited excellent endurance in a vacuum and maintained high capacity and voltage at the end of the discharge. The reliable cycling of the PE cell in a vacuum was attributed to the adhesive properties of the gel electrolyte that held the laminate film package and active electrode materials together. A comparison of cell performance at various ambient temperatures demonstrated that the proper ambient temperature range for a PE cell is from 10 to 30 °C.


*Keywords:* Laminated lithium-ion cell; Polymer electrolyte; Liquid electrolyte; Satellite application; Cycle-life testing; Vacuum

## 1. Introduction

The rapid progress in commercial and consumer microelectronics has catalyzed the use of microsatellites in both civil and military missions, including specialized communications services and research, earth observation and remote sensing, small-scale space science, technology demonstration and verification, and education and training [1–5]. These microsatellites, with a mass ranging from 10 to 100 kg and a designed mission life of less than 1 year, play a role complementary to traditional large satellites operating in a low earth orbit (LEO) by providing an alternative gap-filler for affordable, quick response and exploratory missions with very real and beneficial advantages in terms of cost and response time. However, the limited payload mass, volume, and power in a microsatellite necessitate small, lightweight, inexpensive onboard components. This is particularly true for the rechargeable battery system, which is generally one of the most massive onboard components [6–8].

Nickel–cadmium (Ni–Cd) and nickel–hydrogen (Ni–$H_2$) batteries have primarily been used for power storage in space. However, lithium-ion cells exhibit attractive characteristics of higher energy density, higher working voltage, lower self-discharge, and no memory effect, and thus lithium-ion batteries are expected to replace conventional alkaline batteries [9–14]. Laminated lithium-ion cells in particular, which use aluminum laminate film as package material, may be configured with great flexibility to meet various system demands. These advantages allow for different design approaches for the power storage systems of satellites compared with established space engineering techniques. For example, aluminum tape may be used as a simple means to affix the cells. This renders battery stacking unnecessary and results in high energy density of the battery. Additionally, the thin-layer structure of laminated lithium-ion cells enables them to be inserted between the onboard instruments without requiring a specially designated location. For these reasons, laminated

* Corresponding author. Tel.: +81 29 868 4247; fax: +81 29 868 5969.
*E-mail address:* oh.kenmei@jaxa.jp (X. Wang).

0378-7753/$ – see front matter © 2004 Elsevier B.V. All rights reserved.
doi:10.1016/j.jpowsour.2004.08.021

lithium-ion cells are particularly appealing for microsatellite applications.

We conducted a flexibility evaluation of commercial laminated lithium-ion cells 3 years ago at the Japan Aerospace Exploration Agency (JAXA, formerly National Space Development Agency of Japan) to facilitate the application of laminated lithium-ion cells in microsatellites. We summarized the cycle-life testing of these cells in previous papers by simulating LEO operation with a 40% depth of discharge (DOD) profile [15–18]. After then, we further focused specifically on the cycle-life testing of laminated lithium-ion cells in a vacuum. This paper reports the most recent results.

Laminated lithium-ion cells use aluminum laminate packages, and thus we must first determine whether these cells cycle normally in a vacuum. Commercial laminated lithium-ion cells are generally divided into two types according to their electrolyte states. One type is the common lithium-ion cell with liquid electrolyte, designated here as the liquid-type electrolyte (LE) cell. The other type is a lithium-ion polymer cell, which contains polymer support material to form gel electrolytes by incorporating organic electrolytes, designated here as the polymer-type electrolyte (PE) cell. The different adhesive properties of polymer and liquid electrolytes in laminating film packages enable us to easily deduce that the electrolyte state may affect the endurance of laminated lithium-ion cells in a vacuum. Therefore, it should be very interesting to compare the cycling behavior of the cells containing liquid and polymer by simulating LEO satellite operation in a vacuum. No previous data is available on this aspect.

Our primary objective was to evaluate the effect of a vacuum on the cycling behavior of laminated lithium-ion cells with a liquid-type electrolyte, and laminated lithium-ion cells with a polymer-type electrolyte, both manufactured by the same company and with equal nominal capacity. We tested the cycle life of LE and PE cells in a simulated LEO satellite operation with a 40% DOD profile and compared their cycling performance to achieve this objective. We also investigated the effect of ambient temperature on the cycling behavior of these cells.

## 2. Experimental

### 2.1. Sample of laminated lithium-ion cells

Table 1 lists typical properties of both types of laminated lithium-ion cells evaluated in this work. These cells, also manufactured by the same company, have similar properties except for the electrolyte state. We attribute the difference in cycling behavior of LE and PE cells to the electrolyte state effect. According to the shipment check data from the manufacturer, the ambient temperature tolerance for both cells ranges from 0 to 45 °C.

### 2.2. Vacuum chamber and cell setup

Fig. 1 depicts the cell setup in a vacuum chamber. The vacuum chamber has a capacity of about 20 Pa, maintained by continuous operation of a rotary vacuum pump. We tested two cells of each electrolyte type (LE1 and LE2, PE1 and PE2) under identical conditions to determine their performance dispersion. We used aluminum tape to affix the cells onto the copper plate of the vacuum chamber. This is the same procedure expected for use in affixing laminated lithium-ion cells in a real microsatellite. A thin layer of silicon grease (Sunhayato, SCH-20) applied between the cells and the copper plate improved the radiation of heat.

The vacuum chamber was initially maintained at normal atmospheric pressure for testing then subsequently decompressed to approximately 20 Pa after 300 cycles to simulate a vacuum. The ambient temperature of the cells was maintained between 0 and 45 °C via a water-flow thermostat in a copper plate.

### 2.3. Cycle-life testing

We tested the cycle life of each cell individually using a Charge–Discharge Battery Tester (Kikusui, PFX-2000). We monitored cell voltage, cell current, cell temperature, copper plate temperature, and pressure in the vacuum chamber during the testing.

#### 2.3.1. Charge–discharge cycle

We tested cells by simulating a satellite's LEO operation with a DOD of 40% under a regimen of constant-current, constant-voltage (CC–CV) charge, and constant-current (CC) discharge. We charged the cells with a taper voltage of 4.1 V, a total charge time of 6 h, and a charge rate of 0.5 C at the beginning of the cycle-life testing. We charged the cells for 60 min in every charge–discharge cycle at a taper voltage of 4.1 V and a charge rate of 0.5 C, and we discharged them for 30 min at a discharge rate of 0.8 C. We determined the cycle life based on the cycle at which voltage in the discharge phase dropped to 2.75 V. The charge current was calculated here by using the nominal cell capacity.

Table 1
Typical properties of the laminated lithium-ion cells evaluated in this work

| Sample | Electrolyte | Nominal | | Size[a] (mm) | | | Weight[a] (g) |
|---|---|---|---|---|---|---|---|
| | | Capacity (A h) | Voltage (V) | Length | Width | Thickness | |
| LE | Liquid | 0.68 | 3.7 | 61.0 | 35.0 | 3.8 | 14.33 |
| PE | Polymer | 0.65 | 3.7 | 53.8 | 40.6 | 3.8 | 14.91 |

[a] Average value.

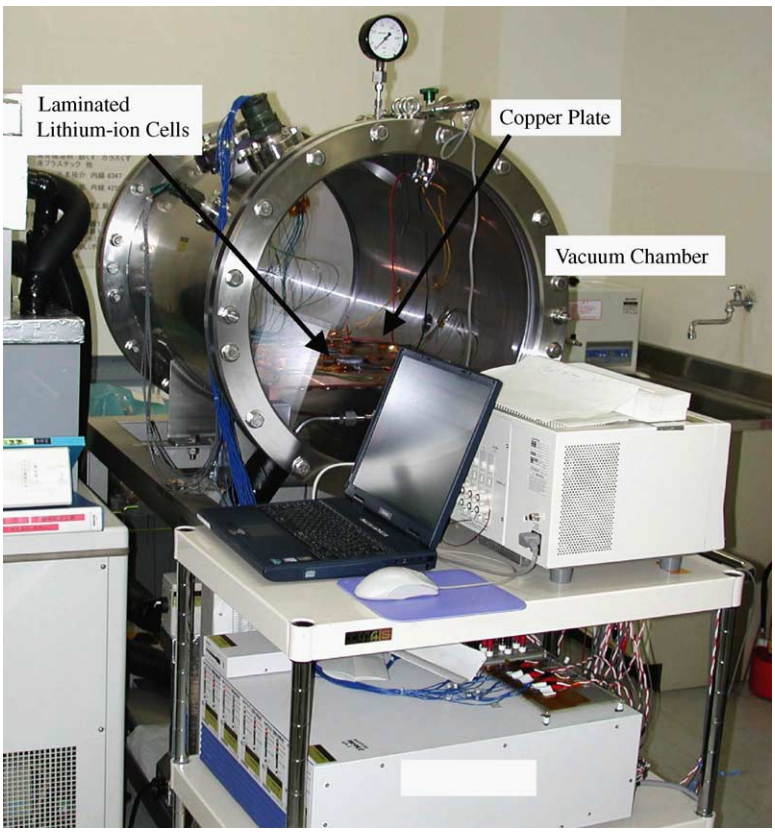


Fig. 1. Photograph of laminated lithium-ion cells set in a vacuum chamber. Aluminum tape was used to affix the cells to the copper plate.

*2.3.2. Capacity verification*

We verified the residual and real capacity of every cell at fixed points during the cycle-life testing. We measured the residual capacity after charging the cells under cycle-life testing conditions by directly discharging the cells in CC mode at a rate of 0.5 C with a cut-off voltage of 2.75V. We charged each cell again in CC–CV mode at a rate of 0.5 C with a taper voltage of 4.1 V for 6 h, and then discharged them under the same conditions we used for the residual capacity. The capacity we obtained was defined as the real capacity.

*2.3.3. Impedance measurement*

We left the cell in an open-circuit state for at least 1 h after every capacity verification to stabilize the cell voltage. We then measured the ac impedance at frequencies from 0.01 Hz to 10 kHz at 5 mV potentiostatic signal amplitude using a Solartron FRA 1255B frequency-response analyzer and a Solartron model 1287 electrochemical interface.

## 3. Results and discussion

### *3.1. Cell appearance*

Batteries for space applications are used in a vacuum, and therefore laminated lithium-ion cells must function normally in such an environment. We first investigated the effect of a vacuum on cell appearance in this study.

Fig. 2 depicts an example of a PE cell before and after a vacuum was applied. No change in outward appearance of the PE cell was observed in the vacuum, indicating proper endurance of the PE cell.

In contrast, the LE cell greatly expanded in the vacuum when compared to its operation in normal atmosphere, as illustrated in Fig. 3. As a result, the aluminum tape used to fix the cell peeled off the copper plate, exposing the white silicon grease between the cell and the copper plate. In a normal atmosphere, the aluminum tape may be enough to fix LE cells. However, the LE cells experienced serious expansion in a vacuum, as seen in Fig. 3. As a result, the aluminum tape could not keep the LE cells in the original position. This is very dangerous for those cells used as satellite's power because they are required to endure the severe shock and vibration during satellite launching. Therefore, the results obtained in Fig. 3 suggest that aluminum tape is unsuitable for laminated lithium-ion cells with liquid electrolyte for vibration and shock endurance during launching.

We sequentially altered the ambient temperature of the copper plate after 1300 cycles from the initial 20 to 10, then 20, 0, 5, 20, 30, 20, 45, and back to 20 °C to investigate the ambient-temperature effect on cell performance. The PE cell retained its initial appearance at an ambient temperature below 30 °C. However, we observed a slight

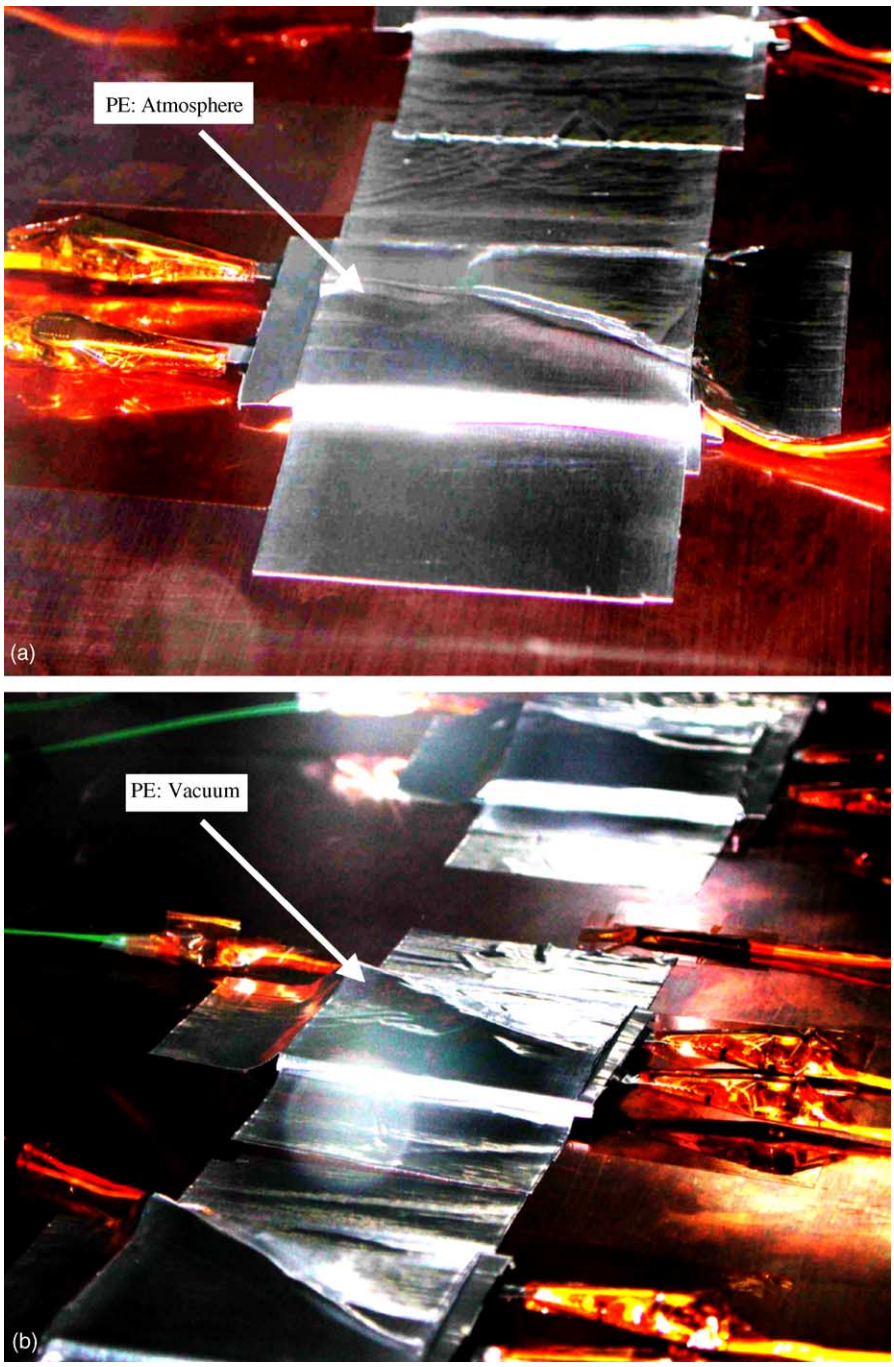


Fig. 2. Appearance of a PE cell with a polymer-type electrolyte (a) before and (b) after we applied the vacuum. Image in (b) was taken in the direction opposite to that in (a). We observed no obvious change in appearance.

expansion of this cell when the ambient temperature rose to 45 °C, the maximum tolerance temperature for the PE cell. This expansion could not be entirely reversed even after the ambient temperature was returned to 20 °C. One possible explanation for this is that part of the electrolyte underwent an irreversible reaction accompanied by gaseous product(s) at 45 °C. This suggests that the PE cell should be operated at an ambient temperature below 45 °C, preferably at 30 °C.

### 3.2. Cycle-life testing

The LE cell and PE cell exhibited different charge and discharge characteristics both before and after the vacuum that corresponded to the changes in appearance, as described below.

The voltage at the end of the discharge is generally an important parameter in comparing the cycling performance of cells. High voltage at the end of the discharge is necessary

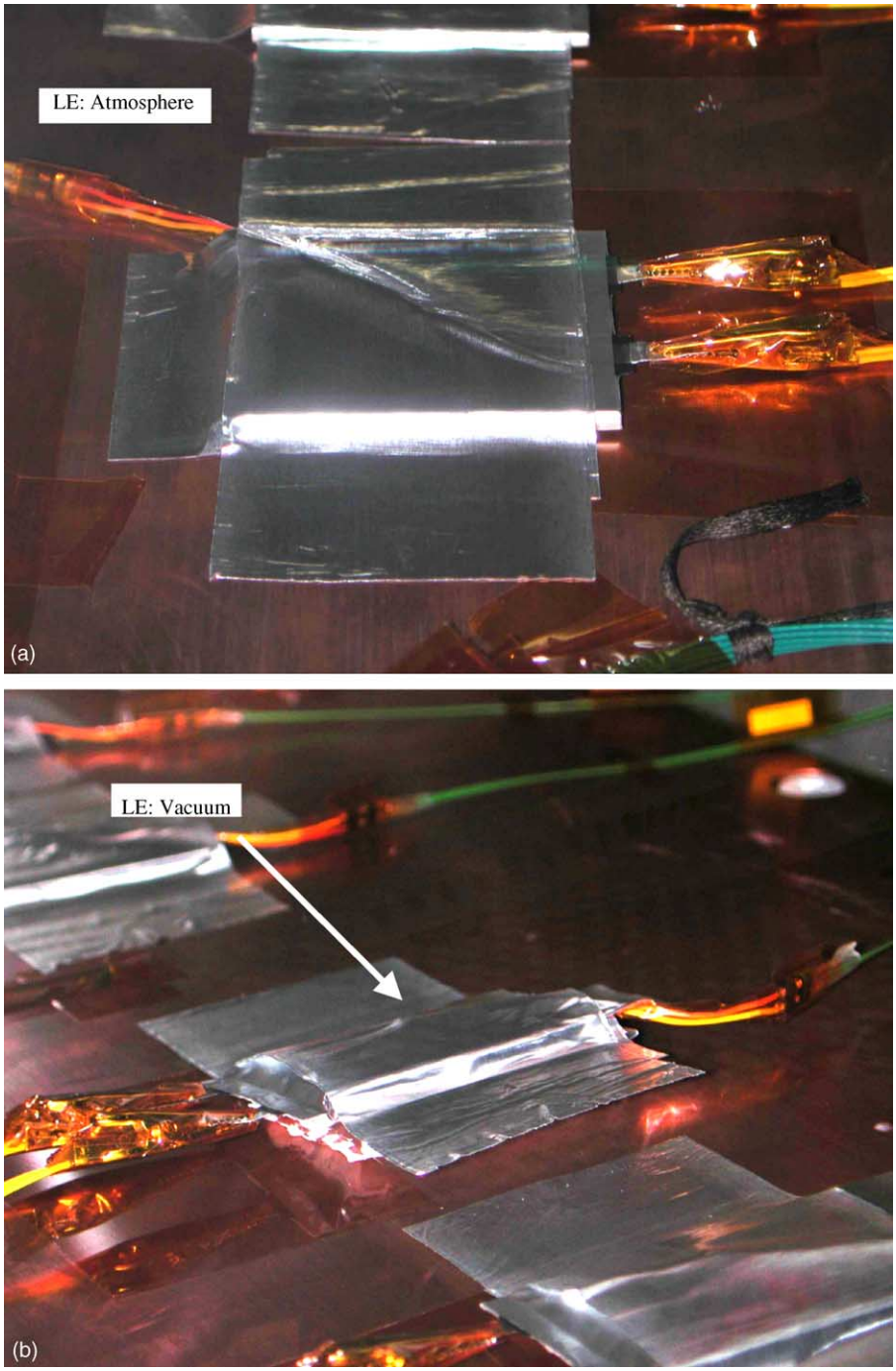


Fig. 3. Appearance of a LE cell with a liquid-type electrolyte (a) before and (b) after we applied the vacuum. Image in (b) was taken in the direction opposite to that in (a). The cell expanded in the vacuum.

for long-term satellite operation. The voltage curves of the two cells are presented in Fig. 4 as an example. The discharge curve of cycle 299 for the PE cell in a normal atmosphere was nearly the same as that of cycle 307 in a vacuum. However, the discharge curve of cycle 307 for the LE cell in a vacuum was severely degraded compared with that in a normal atmosphere.

Cycling further verified this tendency. Fig. 5 presents the voltage trends at the end of both the charge and discharge of the LE and PE cells. We completed 4000 cycles, corresponding to about 8 months of LEO satellite operation. The LE cell exhibited higher voltage than the PE cell at the end of the discharge in a normal atmosphere before cycle 300; however, the vacuum after cycle 300 led to a severe voltage decline for the LE cell at the end of the discharge. As a result, the voltage at the end of the discharge for the PE cell was greater than that of the LE cell after approximately 1000 cycles. A comparison of the voltage trends at the end of the

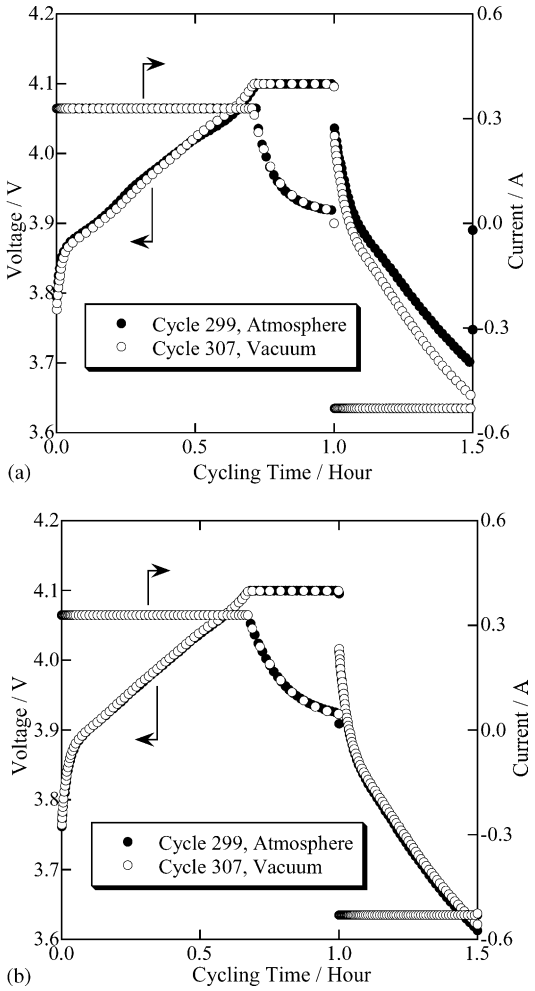


Fig. 4. Voltage and current curves of (a) LE and (b) PE cells before and after we applied the vacuum. The LE cells underwent a voltage decline at the end of the discharge due to the vacuum. We observed no voltage change for the PE cells.

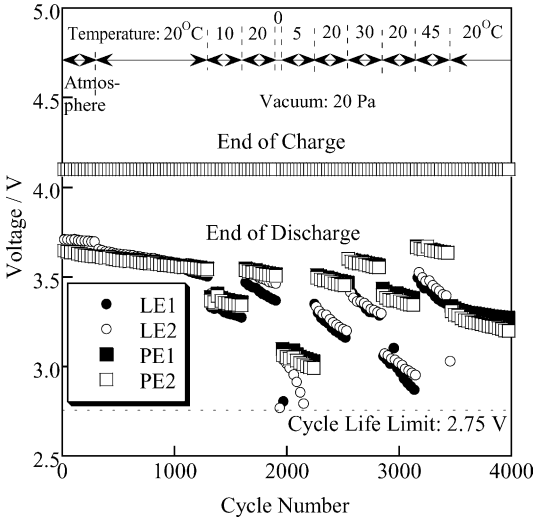


Fig. 5. Voltage trends at the end of the charge and discharge of the LE and PE cells. The chamber environment and ambient temperature are indicated in the graph. The PE cell exhibited acceptable cycling performance in an ambient temperature range from 10 to 30 °C.

discharge indicated that the PE cells had lower performance dispersion than the LE cells.

Fig. 5 also illustrates the ambient-temperature effect on cell performance. Three conclusions can be drawn here. First, the PE cell may be cycled at an ambient temperature as low as 5 °C, even though we observed a greater voltage decline at the end of the discharge at a low ambient temperature. Second, a high ambient temperature is appropriate for PE cell operation within the limits of the 300-cycle data at each ambient temperature. Third, the PE cell maintained a high voltage of about 3.2 V at the end of the discharge, even after 4000 cycles. On the other hand, when the ambient temperature returned to the standard 20 °C after the 3400th cycle, the voltage of the LE cell declined to below the lower voltage limit of 2.75 V at the end of the discharge when the cycle-life testing was finished.

Fig. 4 also shows the current curves of LE and PE cells. In the CV phase, the cell current diminished with charge time at the taper voltage. This decrease in charge current depends entirely on the cell internal impedance. The lower the cell internal impedance, the lower the current at the end of the charge. From Fig. 4, one can deduce that the cell internal impedance of both LE and PE cells increased with cycling.

Fig. 6 indicates the current trend at the end of charging the LE and PE cells. A comparison of the trends in the current of the LE and PE cells revealed that the LE cell had a lower current at the end of the charge than the PE cell before cycle 2200, even though a vacuum was applied after cycle 300. This demonstrates that it is difficult to attribute voltage decline at the end of the discharge only to an increase in the cell internal impedance. There are other factors that result in a decline in cycling performance of a LE cell in a vacuum. The current at the end of the charge for the PE cell was lower after cycle 2200 than that of the LE cell.

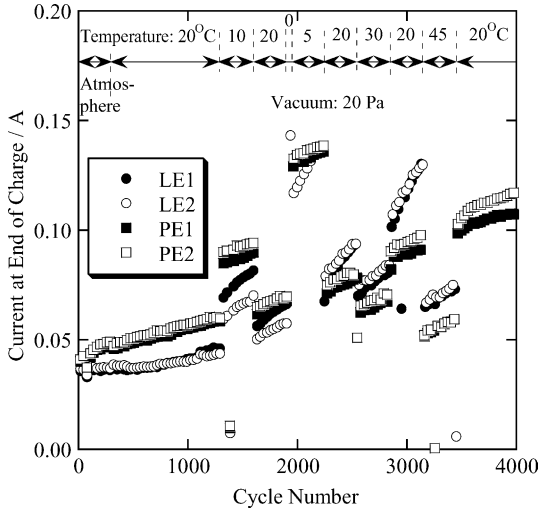


Fig. 6. Current trend at the end of the charge of the LE and PE cells. With cycling, the LE cell had a bigger current increase at the end of the charge than that of the PE cell.

The cell capacities were verified at fixed points during the testing. Fig. 7 presents the changes in the residual and real capacities of both the LE and PE cells. The much longer charge time applied in the real capacity measurement caused the difference between the residual and real capacities. This difference reflects the capacity loss during testing due to the cell internal impedance. The difference between the residual and real capacities increased with cycling for the LE cell, and the real capacity decreased sharply after a vacuum was applied. This correlates with the voltage decline at the end of the discharge, as illustrated in Fig. 5. The PE cell exhibited a gentle decline in real capacity and a relatively small difference between the residual and real capacities, yielding an acceptable cycling performance for this type of cell.

The capacity ratio of the charge and discharge (C/D ratio) is another important parameter that reflects the difficulty of cell capacity recovery in the charging process. Fig. 8 presents

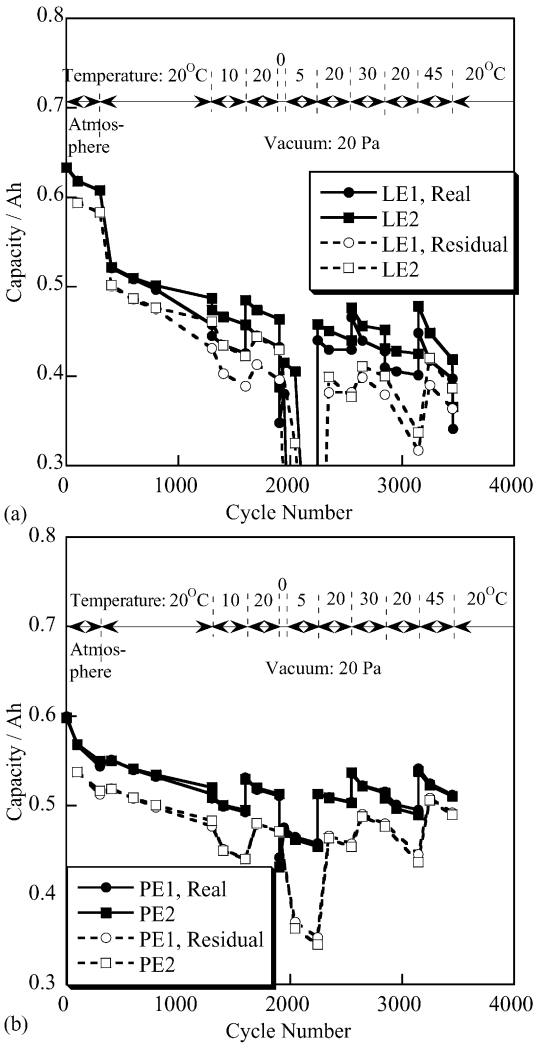


Fig. 7. Change in the residual and real capacities of (a) LE and (b) PE cells. The chamber environment and ambient temperature are indicated in the graph. The PE cell exhibited relatively good capacity retention even in the vacuum.

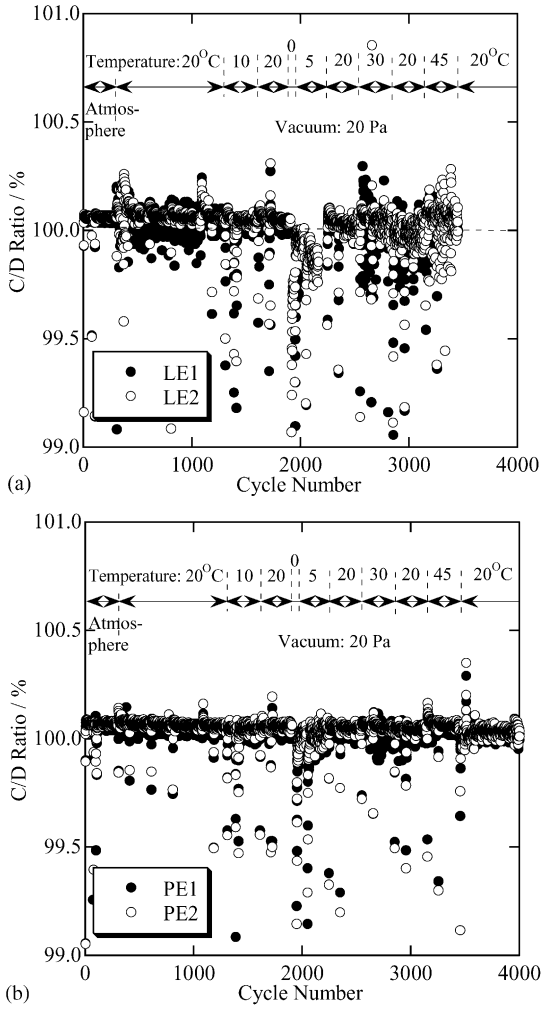


Fig. 8. Capacity ratio of charge and discharge (C/D ratio) of (a) LE and (b) PE cells. We observed a considerable fluctuation around the base value of 100% in the C/D ratio for LE cells after a vacuum was applied.

the C/D ratio of these cells up to 4000 cycles. The C/D ratio decreased with cycling, indicating that the difficulty of cell-capacity recovery in the charging process increases with cycling. Additionally, we can deduce that the decline in the C/D ratio is attributable to an increase in cell impedance since the C/D ratio depends heavily on the ambient temperature. The LE cell exhibited a considerable fluctuation around the base value of 100% in the C/D ratio in a vacuum. A particularly severe insufficiency in the charge capacity of the LE cell occurred after cycle 2400, even at an ambient temperature of 20 °C, corresponding to the voltage decline at the end of the discharge.

The above results indicate that the cell internal impedance is an important factor that affects its cycling performance. We measured the cell impedance after each capacity verification to clarify this correlation. Fig. 9 depicts representative Cole–Cole plots of the LE and PE cells at 20 °C. Two separate semicircles may be distinguished at medium frequencies. In the low-frequency range, a straight line was observed, reflecting the lithium-ion diffusion process in electrode active

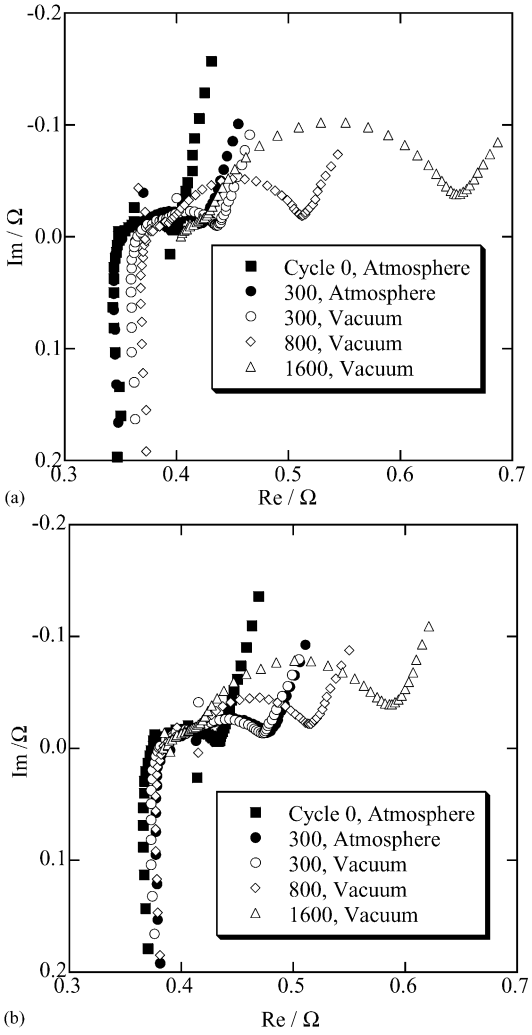


Fig. 9. Cole–Cole plots of (a) LE and (b) PE cells at 20 °C.

materials. Furthermore, we found that the semicircle in the high-frequency range was almost constant with SOC, in contrast to the semicircle in the middle-frequency range. Many works have been done to interpret the impedance of a lithium-ion cell [19,20]. Generally, we could accept that the contribution to cell impedance from the anode appeared only at high frequencies, while the impedance at moderate to low frequency was due to the cathode. By using this knowledge, we deduced from Fig. 9 that the cathode, rather than the anode or electrolyte largely dictated the cell impedance.

The intercept with the reality axis for the LE cell, corresponding to the connection resistance of the current collector and electrolyte, increased steeply due to the vacuum after cycle 300, in addition to an increase in the semicircle's diameter at a moderate frequency range reflecting the charge transfer resistance of the cathode. This correlated well with the cell performance decline of the LE cell after the vacuum was applied, as indicated in Figs. 4–7. It is difficult to determine the electrolyte impedance increase caused by a vacuum. Therefore, the preceding result indicates that the cell impedance increase in a vacuum may be attributed to both the charge-transfer resistance of the cathode and to the connection resistance of the current collector. The intercept with the reality axis for the PE cell corresponded to the connection resistance of the current collector and the electrolyte and was almost independent of the vacuum and cycle number. This suggests that the impedance increase resulted primarily from the charge transfer resistance of the cathode.

### 3.3. Discussion

The test results suggest that it is difficult to explain the decline in cycling performance of the LE cell in a vacuum using only the cell internal impedance. We must analyze the relationship of capacity change, cell internal impedance, and voltage trend as described below to understand the different cycling characteristics of LE and PE cells in a vacuum.

The voltage decline at the end of the discharge is attributed primarily to an increase in cell internal impedance and its capacity loss. Although the internal impedance of the LE cell increased after the vacuum was applied at cycle 300, it was still less than that of the PE cell, as indicated in Fig. 9. Furthermore, the increased impedance of the LE cell was partially caused by the connection resistance of the current collector. In contrast, the real and residual capacities of the LE cell simultaneously experienced a steep decrease after cycle 300 (Fig. 7). This suggests that the difference in cycling performance of the LE and PE cells in a vacuum can be explained as follows.

The laminated package expands in a vacuum, leading to exfoliation of the active electrode materials from the current collector and high connection impedance of the current collection, as observed in Fig. 9. The cell's capacity loss increases as a result and its cycling performance decreases. This behavior of the LE cell in a vacuum may be considered to be the primary cause of its poor cycling performance.

In contrast, the PE cell contains polymer support material that forms a gel electrolyte by incorporating organic electrolytes, and therefore both the laminate package and the active electrode materials adhere to the gel electrolyte. This structure maintains the configuration stability of the cell even in a vacuum, and thus contributes to acceptable cycling performance. Actually, we found in a destroyed PE cell that the polymer (gel) electrolyte kept the electrodes and laminate film package together.

In a PE cell, the electrolyte is located in the hole of polymer material. Since the polymer structure keeps stable in a vacuum, the electrolyte distribution is also stable. On the other hand, LE cell expands in a vacuum. This may lead to the electrolyte evaporation, and hence cell impedance increase, as shown in Fig. 9a.

The capacity loss of a LE cell in a vacuum may be reversed when the cell re-enters a normal atmosphere again due to this incorporating mechanism. We observed this cell capacity increase of a LE cell after changing the chamber environment from a vacuum to a normal atmosphere in another experiment.

This helped confirm the accuracy of our preceding deduction.

In Fig. 5, we found that the PE cells had lower performance dispersion than that of the LE cells. Generally, the voltage decline at the end of the discharge follows the discharge curve of this cell. In the plateau voltage region, the cell voltage is almost independent of cell capacity. Below the plateau voltage, the cell voltage strongly depends on cell voltage. Therefore, the larger the cell-capacity loss, the more serious the cell-performance dispersion may become. In this cycle-life testing, we applied the same depth of discharge and taper voltage in every cycle. The voltage decline at the end of the discharge was mainly attributable to capacity loss during the cycling. As shown in Fig. 7, PE cells had better capacity retention and capacity dispersion than LE cells in a vacuum, which led to less voltage dispersion of PE cells than LE cells.

The ambient temperature plays an important role in determining the cycling performance of a lithium-ion cell. Conventional alkaline cells for space applications generally require an ambient temperature ranging from 0 to 10 °C to achieve the best cycling performance. The operation temperature range must also be optimized for lithium-ion cells used as satellite power sources. A laminated lithium-ion cell may be inserted in the onboard instruments of a microsatellite, as stated above. As a result, the thermal properties of the instruments may severely affect the ambient temperature of the laminated lithium-ion cell. Laminated lithium-ion cells are generally sensitive to high temperature due to the use of a laminate film package, which may lead to organic electrolyte vaporization and hence to cell expansion. However, too low an ambient temperature causes poor cycling performance due to the cell's high internal impedance. The voltage trend in Fig. 5 indicates that the proper ambient temperature for a PE cell is from 10 to 30 °C, while the lower limit of the ambient temperature is 5 °C to enable normal cycling of this cell.

Microsatellites using commercial lithium-ion cells require an approach very different from established space techniques. A microsatellite operates in LEO and is generally designed for a short mission life, usually less than 1 year. This enables use of lithium-ion cells under relatively strict conditions, such as a high charge rate, high taper voltage, and a wider range of ambient temperature. Sample screening and simulated cycle-life testing for new technologies became significant for commercial lithium-ion cells to keep pace with the rapid changes in the commercial market. We must verify the endurance of laminated lithium-ion cells in space to facilitate their application to microsatellites. This encourages testing of vacuum vibration and off-gas testing in a vacuum, as our next step.

## 4. Conclusions

We are testing the cycle life of commercial laminated lithium-ion cells with both liquid and polymer electrolytes by simulating a satellite's LEO operation in various environmental conditions at JAXA, with the objective of microsatellite application. We have completed 4000 cycles, corresponding to about 8 months of LEO satellite operation.

The LE cells initially exhibited better performance than the PE cells in a normal atmosphere. However, the LE cell began to expand in the vacuum environment (about 20 Pa), accompanied by capacity loss and voltage decline at the end of the discharge cycle. In contrast, the PE cells exhibited excellent endurance in a vacuum and maintained high capacity and high voltage at the end of the discharge cycle. We interpreted this difference in cell performance of LE and PE cells to be based on their individual electrolyte properties. We attribute the acceptable cycling behavior of the PE cell in a vacuum to the adhesive properties of the gel electrolyte that holds the laminate film package and the active electrode materials together. A comparison of cell performances at various ambient temperatures demonstrated that the proper ambient temperature range for this cell is from 10 to 30 °C.

## Acknowledgements

The authors thank Mr. Noriyuki Tsubaki, Mr. Yasuhiro Yoshioka, Mr. Toshio Igarashi, Mr. Hiroki Sugiyama and Mr. Makoto Matsuda of Ryoei Technica Corporation, for technical support in this work.JAXA assisted in meeting the publication costs of this article.

## References

[1] F. Buission, Proceedings of the 52nd International Astronautical Congress, International Astronautical Federation, Rio de Janeiro, Brazil, 2001.
[2] M. Parot, P. Ultre-Guerard, T. Cussac, Proceedings of the 52nd International Astronautical Congress, International Astronautical Federation, Rio de Janeiro, Brazil, 2001.
[3] S. Feng, D. Qin, Proceedings of the 50th International Astronautical Congress, International Astronautical Federation, Amsterdam, The Netherlands, 1999.
[4] A.D. Ketsdever, J. Womg, H. Reed, Proceedings of the 36th AIAA/ASME/SAE/ASEE Joint Propulsion Conference and Exhibit, Huntsville, Alabama, July 16–19, 2000.
[5] D. Loche, J.-M. Dubouch, A. Lehman, Proceedings of the Fifth European Space Power Conference, ESA SP-416, Tarragona, Spain, 1998.
[6] J.K. McDermott, in: J.R. Wertz, W.J. Larson (Eds.), Space Mission Analysis and Design, third ed., The Space Technology Library, California, 1999, p. 407.
[7] S. Kuwajima, Battery technology, in: Yuichi Sato (Ed.), The Committee of Battery Technology, vol. 14, The Electrochemical Society of Japan, Tokyo, 2002.
[8] P. Cowles, D. Lizius, R. Spurett, C. Thwaite, M. Slimm, Proceedings of the 18th AIAA International Communication Satellite Systems Conference and Exhibit, AIAA, Oakland, USA, 2000.
[9] T. Inoue, T. Sasaki, N. Imamura, H. Yoshida, M. Mizutani, Proceedings of the 2001 NASA Aerospace Battery Workshop, Marshall Space Flight Center, Huntsville, USA, 2002 (CD-ROM version).
[10] Y. Borthomieu, Proceedings of the 1999 NASA Aerospace Battery Workshop, Marshall Space Flight Center, Huntsville, USA, 2000 (CD-ROM version).

[11] H. Croft, B. Staniewicz, Proceedings of the 2001 NASA Aerospace Battery Workshop, Marshall Space Flight Center, Huntsville, USA, 2002 (CD-ROM version).
[12] B.V. Ratnakumar, M.C. Smart, A. Kindle, H. Frank, R. Ewell, S. Surampudi, J. Power Sources 119–121 (2003) 906.
[13] J.P. Fellner, G.J. Loeber, S.P. Vukson, C.A. Riepenhoff, J. Power Sources 119–121 (2003) 911.
[14] M.C. Smart, B.V. Ratnakumar, S. Surampudi, J. Electrochem. Soc. 146 (1999) 486.
[15] X. Wang, Y. Sone, H. Kusawake, K. Kanno, S. Kuwajima, Proceedings of the 2002 NASA Aerospace Battery Workshop, Marshall Space Flight Center, Huntsville, USA, 2003 (CD-ROM version).
[16] X. Wang, Y. Sone, C. Yamada, S. Kuwajima, Proceedings of the 2003 NASA Aerospace Battery Workshop, Marshall Space Flight Center, Huntsville, USA, 2004 (CD-ROM version).
[17] X. Wang, Y. Sone, S. Kuwajima, J. Electrochem. Soc. 151 (2004) A273.
[18] X. Wang, Y. Sone, S. Kuwajima, J. Power Sources (Submitted for publication).
[19] B.A. Johnson, R.E. White, J. Power Sources 70 (1998) 48.
[20] J. Baker, R. Pynenburg, R. Koksbang, M.Y. Saidi, Electrochim. Acta 41 (1996) 2481.